Design of a Ka-Band Gyro-TWT for Radar Applications

Khanh T. Nguyen, Jeffrey P. Calame, Dean E. Pershing, Bruce G. Danly, Morag Garven, Baruch Levush, *Senior Member, IEEE*, and Thomas M. Antonsen, Jr., *Member, IEEE*

***Abstract*—The design of a Ka-band gyrotron traveling wave tube (TWT) amplifier capable of operating over a wide range of peak powers and bandwidths is presented. The amplifier operates in the TE_{11} mode at the fundamental cyclotron harmonic. Instantaneous bandwidths in the range of 2.5 to 3.9 GHz (at 1 dB below saturation) with corresponding peak powers between 92.2 and 57.9 kW can be achieved by simply adjusting the mod-anode voltage of the electron gun. The corresponding gains range from 57.1 to 36.0 dB. The design performance is obtained with a high quality, 6 A, 70 kV electron beam generated with a double-anode magnetron injection gun. This wide range performance capability in the design is achieved via the use of the distributed loss approach in the interacting circuit, which also guarantees zero-drive stability. A diffractive loading scheme is employed in the lossy section of the circuit to ensure high average power operation of the amplifier.**

***Index Terms*—Gyro-amplifiers, gyrotron traveling wave tube, magnetron injection gun, radars.**

I. Introduction

EXTENDING the bandwidth and average power capability of vacuum electron devices for the next generation of millimeter wave radars is a major research goal at the Naval Research Laboratory. Gyro-amplifiers such as the gyroklystron and gyrotron traveling wave tube (gyro-TWT) appear to be ideal candidates for this purpose due to their high power handling capability (at high frequency) relative to their conventional counterparts, i.e., klystrons [1], [2] and coupled-cavity TWTs [3]. This paper presents the design of a high-average power compatible, Ka-band gyro-TWT. This amplifier design employs the circular TE_{11} mode and operates at the fundamental cyclotron harmonic. The device is intended to serve as the transmitter power amplifier in radar systems used for a variety of applications, such as precision tracking and high-resolution imaging, etc. These diverse applications have somewhat different requirements in terms of power and bandwidth. Consequently, from a system point of view, it is often desirable to have a high power amplifier that can provide the capability for tailoring the rf characteristics to specific applications. This is the goal of the present amplifier design. In addition to the power-bandwidth extensions, gain flatness across the band is also a consideration for some applications which require a 1 dB bandwidth specification rather than the commonly used 3 dB bandwidth.

Gyro-TWT amplifiers are well known for their wide bandwidth potential. However, for many years, spurious oscillations have been a major obstacle in achieving the high gain and high power potential in gyro-TWTs. These oscillations include the absolute instability at the cutoff frequency of the operating mode, reflective oscillations due to gain exceeding circuit roundtrip return loss, and harmonic gyrotron backward wave oscillations (gyro-BWOs). There is a vast literature associated with the suppression of these oscillations in the development of gyro-TWTs. We refer the readers to the most recent review articles by Granatstein *et al.* [4], Chu *et al.* [5], Felch *et al.* [6], and Nusinovich [7] for more details. Through the course of gyro-TWT development, it was found that the limitation imposed by spurious oscillations could be somewhat alleviated with the use of severs [8]–[10]. In severed gyro-TWTs, the interaction circuit is divided into sections separated by attenuating severs, where each section length is kept below the start-oscillation threshold. However, the gain is still limited due to gyro-BWOs, since the sections are still coupled via the electron beam. Recently, due to the pioneering work of Chu *et al.* [11] at the National Tsing Hua University, Taiwan, this limitation has been essentially removed via the use of a distributed-loss circuit, which consists of a long lossy section combined with a short conducting-wall section at the output end of the device. A saturated gain of 70 dB with 93 kW peak power has been experimentally demonstrated in a fundamental harmonic TE_{11} gyro-TWT using a 3.5 A, 100 kV electron beam with a beam velocity ratio of 1.0. This gain is a 30 dB improvement over that of severed gyro-TWTs [10], and the device is still zero-drive stable. The superiority in gain and stability afforded by the distributed-loss approach provides the necessary margin for the trade-off between gain, bandwidth, and gain flatness called for by the design goal. Thus, the distributed-loss approach is employed in the present amplifier design.

II. Amplifier Design

The design study was performed with the self-consistent, time-dependent, quasi-three-dimensional code, MAGY [12]. MAGY is a versatile design tool and has been used to perform

Manuscript received May 3, 2000; revised September 9, 2000. This work was supported by the Office of Naval Research. The review of this paper was arranged by Editor D. Goebel.

K. T. Nguyen is with the Vacuum Electronics Branch, Naval Research Laboratory, Washington, DC 20375 USA, and also with KN Research, Silver Spring, MD 20905 USA (e-mail: nguyen@mmace.nrl.navy.mil).

J. P. Calame, B. G. Danly, and B. Levush are with the Vacuum Electronics Branch, Naval Research Laboratory, Washington, DC 20375 USA.

D. E. Pershing is with the Vacuum Electronics Branch, Naval Research Laboratory, Washington, DC 20375 USA, and also with Mission Research Corporation, Newington, VA 22122 USA.

M. Garven is with the Vacuum Electronics Branch, Naval Research Laboratory, Washington, DC 20375 USA, and also with Omega-P Inc., New Haven, CT 06520 USA.

T. M. Antonsen, Jr., is with the University of Maryland, College Park, MD 20742 USA.

Publisher Item Identifier S 0018-9383(01)00311-2.

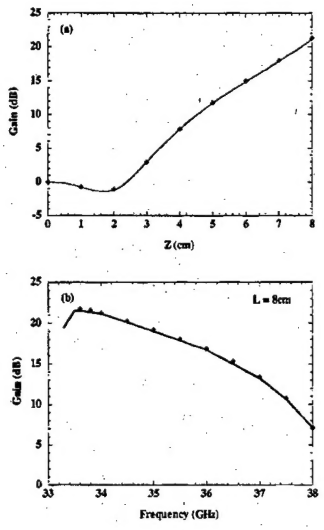

Fig. 1. Comparison between MAGY (solid line) and linear theory (dot) for (a) spatial gain at 34 GHz and (b) total gain for TE_{11} mode in a lossless waveguide of 8 cm long. Beam current, voltage, and velocity ratio are 2.5 A, 65 kV, and 1.0, respectively. Beam guiding center is at 0.35 of waveguide radius (0.2655 cm). Magnetic field is 12.341 kG.

both stability and large signal analyzes. It has been successfully used to design and model gyroklystron amplifiers [13], [14]. To validate the utility of the code for gyro-TWT amplifier design, a battery of simulations was performed for comparison with linear theory predictions. The linear theory prediction is obtained via numerical solutions of the dispersion relation derived by Chu and Lin [15] and later extended by Kuo *et al.*, to include finite boundary conditions [16]. Shown in Fig. 1(a) is a typical comparison between the MAGY predicted linear growth versus axial distance and the linear theory prediction for the TE_{11} mode in a lossless smooth waveguide. The total linear gain for an interaction length of 8 cm is also illustrated in Fig. 1(b). Excellent agreement is evident.

As previously mentioned, harmonic gyro-BWOs are a serious concern in the realization of gyro-TWTs. For TE_{11} gyro-TWT amplifiers, the most troublesome is the second harmonic, TE_{21} gyro-BWO mode [10]. Shown in Fig. 2(a) and (b) are the particle trajectories and power profile as a function of axial distance for the TE_{21} second harmonic gyro-BWO from a MAGY simulation. Note, in particular, the formation of two separated bunches (characteristic of the second harmonic interaction) and the backward flow of the rf power relative to the beam propagation direction. The output power as a function of interaction length is illustrated by Fig. 2(c). This figure indicates that the start oscillation critical length for this mode is at 5.2 cm, which compares well with the linear theory prediction of 5.1 cm. These examples illustrate the utility of MAGY as an appropriate design tool in this application.

The capability of MAGY to accurately predict the start oscillation threshold is critical in designing distributed loss gyro-TWT amplifiers. Unlike severed gyro-TWTs where the beam is the only means of communication between the stages, in distributed loss gyro-TWT amplifiers the rf can also communicate between the loaded and unloaded sections. Thus, the stability analysis in distributed loss gyro-TWTs must be considered on a global scale.

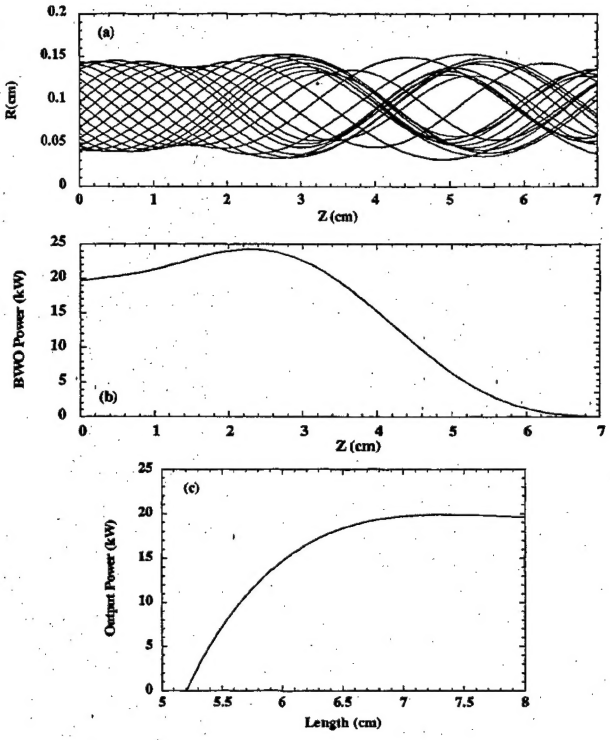

Fig. 2. MAGY simulation of the second harmonic TE_{21} gyro-BWO (~57 GHz) in a lossless waveguide (a) particle trajectories, (b) spatial power profile in a 7 cm circuit, and (c) BWO output power as a function of circuit length. Beam parameters are 6 A, 65 kV, and $\alpha = 1.0$. Magnetic field and circuit radius are 12.341 kG and 0.2655 cm, respectively.

However, in general, linear theory can be used as an aid in the determination of the initial unloaded circuit length. As a rule of thumb, the total length of the unloaded section of the interaction circuit plus one rf-field e-folding length in the loaded section should not exceed the critical length for start oscillation as predicted by linear theory for any problematic modes. As long as this condition is satisfied, the loaded section of the circuit can be made as long as necessary to obtain the required gain. This does not imply that the loaded section can be made arbitrary long since the trade off, of course, is a reduction in bandwidth due to beam velocity spread, particularly, at the high frequency end of the bandwidth.

The circuit geometry of the present design is shown in Fig. 3. This includes the input coupler taper, the uniform interaction circuit, and a nonlinear output uptaper. The collector (not shown) follows the nonlinear output taper and also serves as the rf output waveguide. The interaction circuit radius is 2.72 mm with a total length of 27 cm; the first 22 cm of which have a cold circuit loss of 3.45 dB/cm at 35 GHz for the TE_{11} operating mode. The rf attenuation in the lossy section of the circuit is accomplished via a diffractive coupling technique. This approach permits the aggressive cooling that would be necessary for high average power operation. The desired distributed loss is achieved by using an array of three thin axial slots equally spaced in azimuth (120°). These slots are radial rectangular waveguides through which a fraction of the propagating power is extracted and then dissipated in dielectric loads. It is important to note and easy to show analytically that

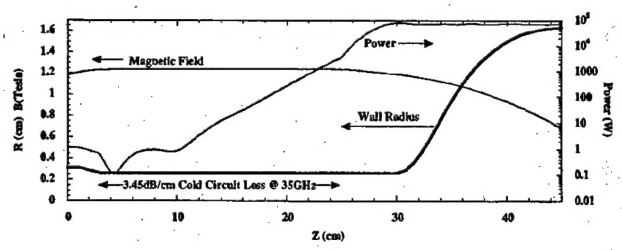

Fig. 3. Circuit geometry and magnetic field profile of the amplifier design. Also shown is the spatial power profile at 35 GHz for a 6 A, 70 kV, $\alpha = 0.7$ electron beam with guiding center radius of 0.121 cm. Interaction circuit radius is 0.272 cm.

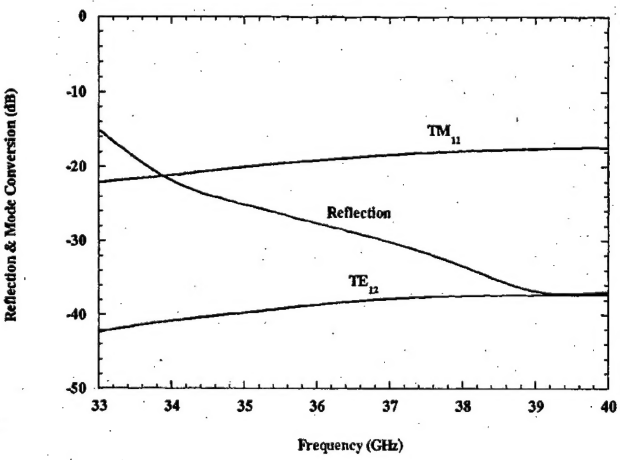

Fig. 4. Return loss and mode conversion of the TE_{11} operating mode to the dominant TE_{12} and TM_{11} modes from the nonlinear uptaper shown in Fig. 3.

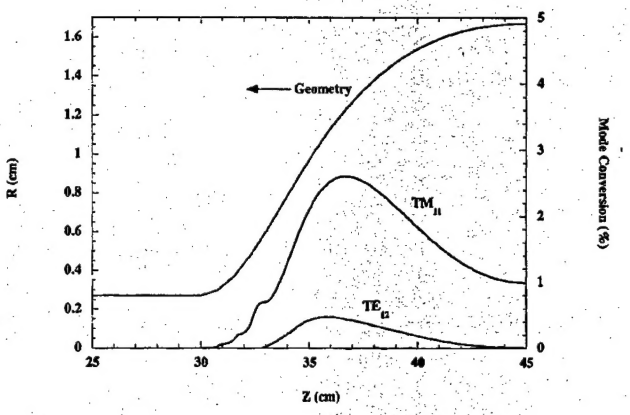

Fig. 5. Axial power profile of the two dominant converted modes at 35 GHz, TE_{12} and TM_{11}, as a percentage of the total power in the nonlinear uptaper. Uptaper profile is also shown for reference.

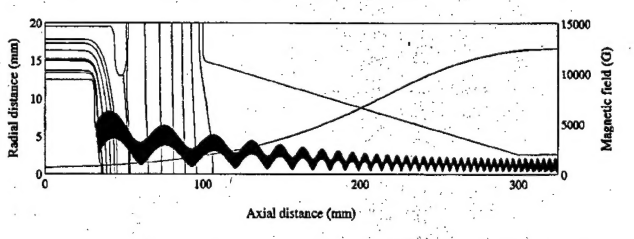

Fig. 6. Electrode profiles, potential contours, magnetic field profile, and particle trajectories of the double-anode magnetron injection gun design.

the use of the three-slot configuration essentially ensures the integrity of the TE_{11} operating mode polarization, which is critical from the beam-wave interaction standpoint. This is also confirmed with simulations using Ansoft's High Frequency Structure Simulator. It should be pointed out that axial slots were first employed in a gyro-TWT by Wang *et al.* [17], to control instabilities but with minimal perturbation to the operating mode. For the present application, in addition to controlling spurious oscillations, the goal is also to attain a specific loss rate for the operating mode. In this context, the loading scheme is more similar to that used in the successful NRL/Industrial high-average power gyro-klystron amplifier [18], [19], though there are significant differences due to the traveling wave excitation of the slots. Further details of the loading scheme will be presented in a future publication. However, we note that the high average power compatible loading scheme employed in the lossy section will also provide approximately 4.25 dB/cm loading for the problematic second harmonic gyro-BWO TE_{21} mode (~56 GHz). Also shown in Fig. 3 is the rf-power profile at 35 GHz for a 6 A, 70 kV, $\alpha = 0.7$ electron beam. The magnetic field profile is also shown in this figure for illustration.

The nonlinear output taper is shaped to minimize reflection of the operating mode and mode conversions. Reflection and mode conversion across the band simulated with MAGY is plotted in Fig. 4. Return loss from the nonlinear output uptaper is better than −20 dB over most of the band, which is necessary to avoid spurious oscillation and also to ensure a reasonably high start oscillation current for the TE_{111} gyro-monotron like mode in the unloaded section of the interaction circuit. This instability has previously been described in [9] and is caused by trapped rf waves between the interface of the loaded and unloaded section on the left and the reflection from uptaper on the right. Consequently, good matching reduces the quality factor of the cavity and, hence, increases the start oscillation current. Also shown in Fig. 4 is the TE_{11} mode conversion into the two dominant modes, TE_{12} and TM_{11}. The axial profile of the power in these modes as a percentage of the total rf power at 35 GHz is plotted in Fig. 5. It is important to note that, at the peak, power in the TE_{12} mode is only 0.5% of the total rf power. This low level of higher order TE mode content reduces the level of excitation of these modes in the nonlinear uptaper due the presence of the modulated beam [14].

The electron beam to be used with this amplifier is produced by a magnetron injection gun (MIG). The MIG was designed using the EGUN trajectory code [20] and employed the same design methodology as described in [21]. Fig. 6 illustrates the electron gun design, which shows the gun electrode profiles, the electron beam trajectory, and the magnetic field profile. The magnetic field is shaped using an existing fourteen coil superconducting magnet and two room temperature gun coils [22]. The nominal beam voltage and current are 70 kV and 6 A, respectively, as tabulated in Table I. The beam velocity ratio, α, is adjusted by varying the mod-anode voltage. This is illustrated by Fig. 7, which shows the beam velocity ratio and perpendicular velocity spread as a function of mod-anode voltage for a

TABLE I
NOMINAL MAGNETRON INJECTION GUN DESIGN PARAMETERS

Beam Current	6 A
Anode Voltage	70 kV
Mod-anode Voltage	24 kV
Velocity Ratio	0.71
Perpendicular Velocity Spread	3.25%
Beam Guiding Center	1.21 mm
Cathode Angle	60^0
Cathode Loading (at 6A)	4.8 A/cm^2
Peak Field Stress	73 kV/cm
Magnetic Compression Ratio	16

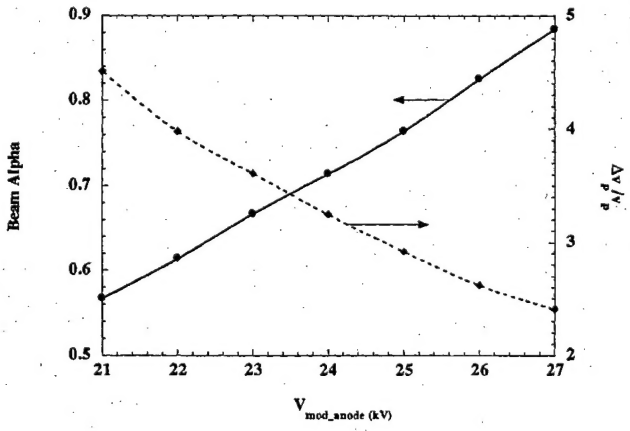

Fig. 7. Beam velocity ratio (solid line) and perpendicular velocity spread (dashed line) as a function of mod-anode voltage for the MIG design shown in Fig. 6.

6 A, 70 kV electron beam. Most of the contribution to the perpendicular velocity spread is induced by phase mixing in the adiabatic compression region. As the beam phase mixes in the presence of the dc space charge, it undergoes a transition from a laminar state, where the space charge potential is axially periodic, to a nonlaminar (completely mixed) state, where the space charge potential is uniform. The spatially periodic space charge field breaks the constancy of the magnetic moment resulting in an increase of the beam velocity spread [23]. This effect is confirmed with the MAG code, which has been developed for analyzing beam velocity spread induced by dc space charge in MIGs [23]. This is shown in Fig. 8, where the evolution of the beam perpendicular spread as a function of axial distance from both EGUN and MAG are compared with good agreement. The beam-guiding center is at 1.21 mm with a magnetic compression ratio of 16. This choice of beam guiding center is a result of a

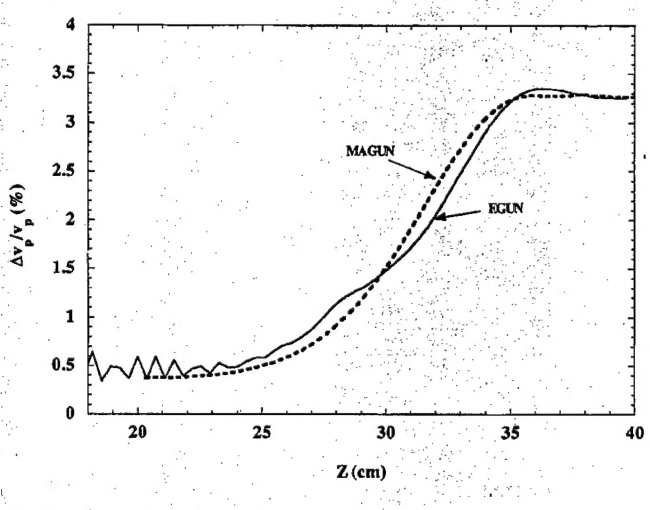

Fig. 8. Comparison of the evolution of the beam perpendicular velocity spread in the adiabatic compression region between EGUN and the space-charge phase mixing code, MAG [19], for the MIG design shown in Fig. 6. Agreement indicates increase is due to space-charge phase mixing. Final beam parameters are 6 A, 70 kV, and $\alpha = 0.7$.

trade off between the beam-wave interaction strength and beam velocity spread. Since space charge phase mixing is a dominant contributor to beam velocity spread, a smaller beam-guiding center results in a larger beam velocity spread, which will adversely impact the amplifier bandwidth.

The lengths of the loaded and unloaded sections of this circuit have been selected to satisfy stability constraints, overall amplifier gain and efficiency requirements, as well as thermal loading issues for high average power operation. For instance, an unloaded section that is too short will reduce the gain, but if too long will reduce the bandwidth due to beam velocity spread. For the loaded section, stability constraints dictate the maximum length, whereas thermal issues and electronic efficiency determine the minimum length. The choice of circuit geometry must also be considered in conjunction with the magnetic field profile and the beam velocity ratios. In general, the higher the beam velocity ratio and magnetic field, such that the beam line approaches or exceeds the grazing (barely touching) intersection with the dispersion line, will lead to higher gain and wider bandwidth. The risk here, of course, is the excitation of the absolute instability as the relativistic cyclotron frequency approaches the cutoff frequency of the operating mode. For the distributed loss scheme, since the loss in the loaded section can greatly increase the start oscillation threshold, this can be advantageously employed. In this particular design, the magnetic field is kept near or slightly above grazing in the relatively long loaded section of the circuit to broaden the rf bandwidth, and the magnetic field is tapered down in the short unloaded section to avoid the onset of instability. Of course, the beam current and velocity ratio must always be selected to satisfy stability criteria globally.

The magnetic field profile employed in the present design is as shown in Fig. 3. The magnetic field strength is 12.1 kG in the loaded section of the circuit (22 cm long). This is followed by a -4% taper in the remaining 5 cm unloaded section of the circuit. At a beam voltage of 70 kV and a circuit radius of 2.72 mm, magnetic field strength of 12.1 kG corresponds to approximately 101, 100, and 99.4% of the grazing magnetic field for

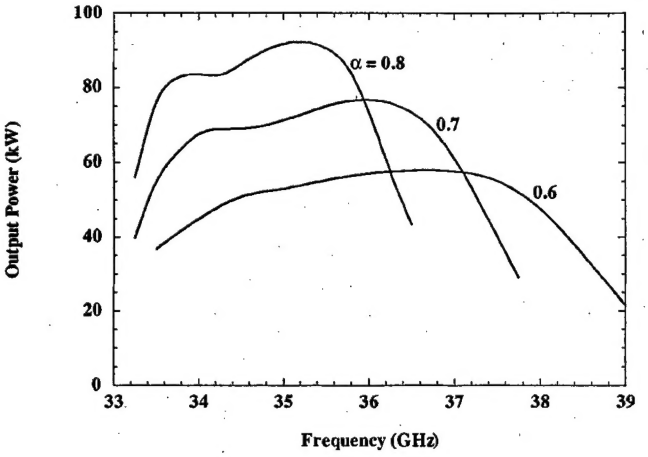

Fig. 9. MAGY predicted constant-drive bandwidths for the gyro-TWT amplifier design with a 6 A, 70 kV electron beam at three different beam velocity ratios for circuit shown in Fig. 3. Assumed beam perpendicular velocity spread is 4%. Input powers are 0.18, 1.8, and 14.5 W for beam velocity ratios of 0.8, 0.7, and 0.6, respectively.

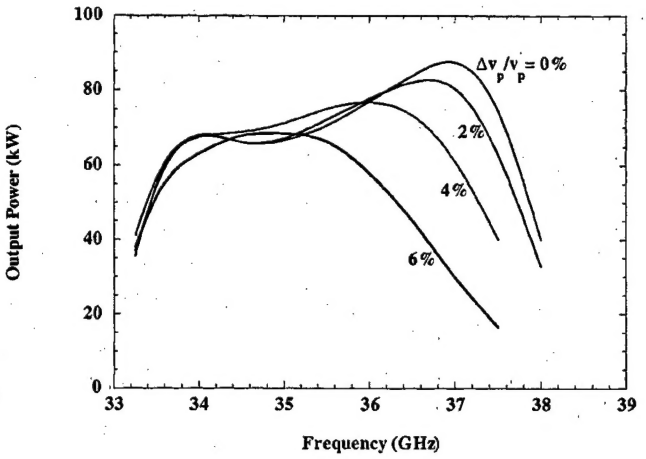

Fig. 10. Effect of beam velocity spreads on amplifier performance for circuit shown in Fig. 3. Beam current, voltage, and velocity ratio are 6 A, 70 kV, and 0.7, respectively. Input power is 1.8 W for all cases.

beam velocity ratios of 0.6, 0.7, and 0.8, respectively. The corresponding rf power profile at 35 GHz for a 6 A, 70 kV, $\alpha = 0.7$ electron beam is also shown in Fig. 3 for illustrative purposes.

The calculated performance for this gyro-TWT design follows. Fig. 9 illustrates the bandwidths for a 6 A, 70 kV beam at three different beam velocity ratios (α) with an assumed perpendicular velocity spread of 4%. The peak output powers are 92.2, 76.8, and 57.9 kW corresponding to electronic efficiencies of 22, 18.3, and 13.8%, for beam velocity ratios of 0.8, 0.7, and 0.6, respectively. The corresponding 1 dB bandwidths are 2.5, 3.3, and 3.9 GHz, respectively, at constant drive powers of 0.18, 1.8, and 14.5 W. It should be emphasized that the bandwidth curves shown in Fig. 9 are obtained by simply changing the beam velocity ratio. This demonstrates the flexibility of this design in selecting the appropriate power/bandwidth characteristics for particular radar applications.

Note that the 1 dB bandwidth is listed above rather than the more typical 3 dB bandwidth. The gain flatness in the present design is achieved by taking advantage of the distributed loss approach, which allows operation near or above grazing in the loaded section without going unstable. As previously mentioned, operation in this regime permits the increased bandwidth. This is especially critical for realistic electron beams with finite velocity spread since velocity spread tends to reduce the gain at the high frequency edge of the band. This is due to the shorter axial wavelength at higher frequencies, which accentuates the negative effects of the beam velocity spread. The overall effect of velocity spread on amplifier bandwidth is illustrated in Fig. 10. In this figure, constant drive (1.8 W) bandwidths for a 6 A, 70 kV electron beam are shown for several perpendicular velocity spreads. As expected, it is readily noted from this figure that the impact of velocity spread at the low frequency edge is minimal and is more pronounced at the high frequency edge. Moreover, it can be observed from this figure that the gain for the high frequency edge in the ideal beam case (no spread) is slightly higher than for the low frequency end. This is a consequence of the choice of the magnetic field profile discussed earlier and, in part, due to the frequency dependence of the loading scheme.

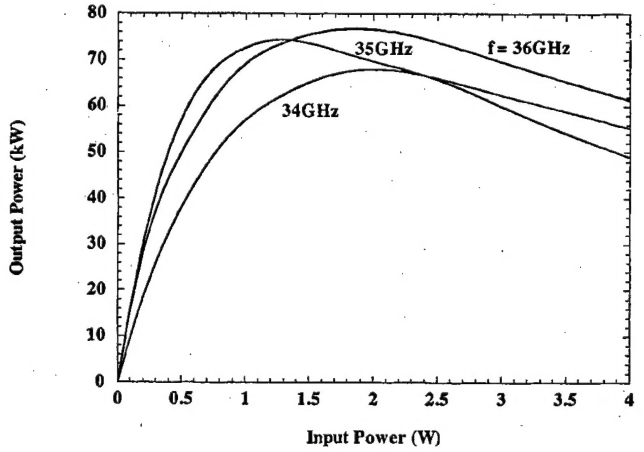

Fig. 11. Drive curves at several frequencies for a 6 A, 70 kV electron beam for circuit shown in Fig. 3. Beam velocity ratio and perpendicular velocity spread are 0.7 and 4%, respectively.

In addition to the velocity spread effects, the bandwidth is also dependent on input power. Specifically, in the gyro-TWT interaction the gain is strongly dependent on the synchronism between the beam and the rf wave. Consequently, the saturated gain at each frequency within the band is different. In general, the closer the synchronism condition is met, the higher the gain. Shown in Fig. 11 are several drive curves at different frequencies for a 6 A, 70 kV electron beam with $\alpha = 0.7$ and a 4% perpendicular velocity spread. It can be seen from this plot that the frequency with the highest saturated gain is 35 GHz, which is the grazing frequency for the unloaded section. This type of plot is quite useful to guide the selection of the correct input power to optimize the power-bandwidth product and the gain flatness. Fig. 12 illustrates the constant drive bandwidths corresponding to Fig. 11 at several input powers. The bandwidth curve for 1.8 W of drive power is the same as that shown in Fig. 9 and is selected for its combined power-bandwidth product and gain flatness.

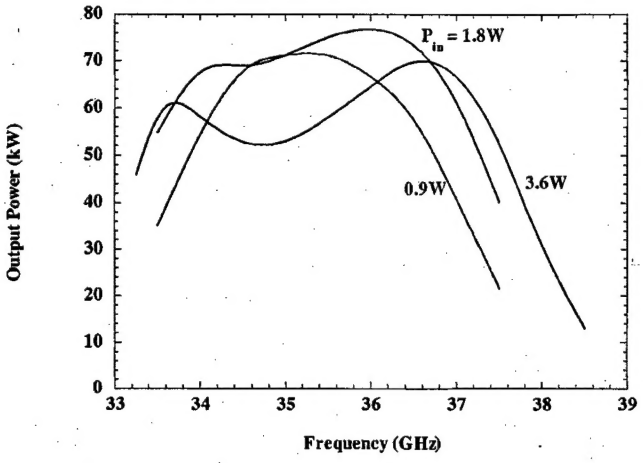

Fig. 12. Constant drive bandwidths for several input powers beam for circuit shown in Fig. 3. Beam parameters are 6 A, 70 kV, $\alpha = 0.7$, and $\Delta v_p'/v_p = 4\%$.

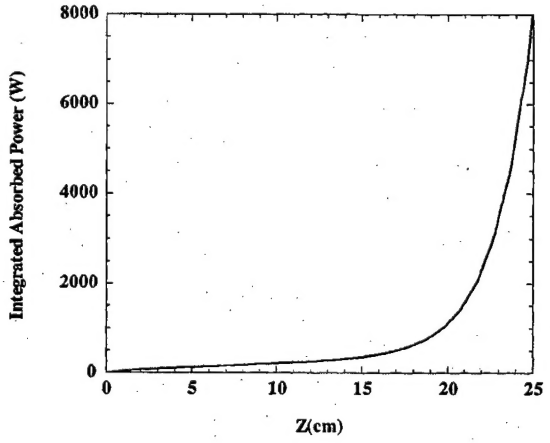

Fig. 13. Spatial profile of integrated rf power absorbed by the load in the lossy section of the saturated amplifier (Fig. 3) at 36 GHz with a 6 A, 70 kV, $\alpha = 0.7$ electron beam. The total peak power absorbed by the load is approximately 8 kW. Most of which is toward the end of the lossy section.

Since the gyro-TWT will be used as the transmitter power amplifier for radar systems, the amplifier must be zero-drive stable at the operating point. This means that rf excitation is absent without drive power. For the magnetic field profile and beam parameters employed in this design, the start oscillation currents for the second harmonic TE_{21} gyro-BWO (~56 GHz) and the reflective TE_{11} oscillation at $\alpha = 0.8$ (the highest velocity ratio employed in the design) are 21 and 11.5 A, respectively, ensuring zero drive stability. At 11.5 A, this threshold is almost a factor of two higher than the design operating current of 6 A. This conservative design provides a safety margin in order to ensure stability in the actual implementation of the amplifier due to uncertainties in load reflections or cold tube loss rates.

A key issue for the amplifier design in the context of high average power operation is the dissipation of the rf power absorbed in the loaded section of the interaction circuit. Since the rf wave grows exponentially, aggressive cooling for the last portion of the loaded section will be required. This is illustrated in Fig. 13, which shows the integrated peak power that must be dissipated in the loaded section for the nominal beam parameters (6 A, 70 kV, 4% perpendicular spread) at 36 GHz. This figure indicates that approximately 1.75 kW of peak rf power must be dissipated in the last 1/2 cm of the loaded section. At 20% duty, this corresponds to greater than 400 W/cm^2 on the circuit wall. For simple copper wall, this level of wall loading can be reasonably cooled with present technology. However, if the loading is achieved with a lossy material coating, thermal cycling fatigue is a serious concern. Furthermore, the loaded region will also act as a heat sink for any reflected rf waves resulting from mismatches downstream from the interaction circuit. For these reasons, a diffractive loading scheme using an azimuthal array of axial slots extracting power to external ceramic loads will be employed as previously mentioned.

III. Summary

In this paper, a Ka-band gyro-TWT design to serve as the transmitter power amplifier for radar systems has been presented. The amplifier will operate in the circular TE_{11} mode at the fundamental harmonic. The design has been performed using the self-consistent three-dimensional code, MAGY. The design has been optimized in terms of power-bandwidth product and gain flatness using the distributed loss approach pioneered by National Tsing-Hua University, Taiwan. To optimize the gain flatness and maximize the output power, a magnetic field at or near grazing is set in the loaded section (22 cm) followed by a -4% taper in the remaining 5 cm of the conducting wall section. Peak powers of 92.2, 76.8, and 57.9 kW have been obtained for a 6 A, 70 kV electron beam with beam velocity ratio of 0.8, 0.7, and 0.6, respectively, assuming a perpendicular velocity spread of 4%. The corresponding 1 dB bandwidths are 2.5, 3.3, and 3.9 GHz, respectively, with gain of 57.1, 46.3, and 36.0 dB. At $\alpha = 0.8$, the start oscillation currents are 11.5 A for the TE_{11} mode and 21 A for the TE_{21} gyro-BWO mode. This conservative design ensures zero drive stability in the actual realization of the amplifier. To accommodate high average power operation, a diffractive loading scheme will be employed.

In conclusion, a high-average-power compatible, Ka-band, gyro-TWT amplifier design for radar applications has been presented. The peak power/bandwidth characteristics can be significantly altered simply by changing the beam velocity ratio. This capability provides the flexibility to tailor the rf output characteristics to any particular radar application.

Acknowledgment

The authors would like to thank Dr. M. Botton for many stimulating discussions.

References

[1] E. L. Wright *et al.*, "Permanent-magnet focused multi-stage depressed collector Klystron amplifiers for satellite communications," in *Proc. Int. Vacuum Electronics Conf.*, Monterey, CA, May 2000, paper 1.4.

[2] Communications & Power Industries, SatCom Division, "Klystron high power amplifiers for SatCom applications," *Microwave J.*, vol. 43, p. 160, 2000.

[3] B. G. James, "Coupled-cavity TWT designed for future MM-wave systems," MSN&CT, Sept. 1986.

[4] V. L. Granatstein, B. Levush, B. G. Danly, and R. K. Parker, "A quarter century of gyrotron research and development," *IEEE Trans. Plasma Sci.*, vol. 25, p. 1322, 1997.
[5] K. R. Chu *et al.*, "Theory and experiment of ultrahigh gain gyrotron travelling wave amplifier," *IEEE Trans. Plasma Science*, vol. 27, p. 391, 1999.
[6] K. L. Felch *et al.*, "Characteristics and applications of fast-wave gyrodevices," *Proc. IEEE*, vol. 87, p. 757, 1999.
[7] G. Nusinovich, "Review of the theory of mode interaction in gyro-devices," *IEEE Trans. Plasma Sci.*, vol. 27, p. 313, 1999.
[8] A. K. Ganguly and S. Ahn, "Large-signal theory of a two-stage wideband gyro-TWT," *IEEE Trans. Electron Devices*, vol. ED-31, p. 474, 1984.
[9] K. R. Chu *et al.*, "Recent developments in millimeter wave gyro-TWT research at NTSU," in *IEDM Tech. Dig.*, 1990, p. 699.
[10] K. R. Chu *et al.*, "Stabilization of absolute instabilities in the gyrotron travelling wave amplifier," *Phys. Rev. Lett.*, vol. 74, p. 1103, 1995.
[11] K. R. Chu *et al.*, "Ultrahigh gain gyrotron travelling wave amplifier," *Phys. Rev. Lett.*, vol. 81, p. 4760, 1998.
[12] M. Botton, T. M. Antonsen, Jr., B. Levush, K. T. Nguyen, and A. N. Vlasov, "MAGY: A time-dependent code for simulation of slow and fast microwaves devices," *IEEE Trans. Plasma Sci.*, vol. 26, p. 882, 1998.
[13] J. P. Calame, *et al.*, "Experimental studies of bandwidth and power production in a three-cavity, 35 GHz gyroklystron amplifier," *Phys. Plasmas*, vol. 6, p. 285, 1999.
[14] K. T. Nguyen *et al.*, "Modeling of gyro-klystrons with MAGY," IEEE Trans. Plasma Science, HPM Special Issue, 2000, to be published.
[15] K. R. Chu and A. T. Lin, "Gain and bandwidth of the gyro-TWT and CARM amplifiers," *IEEE Trans. Plasma Sci.*, vol. 16, p. 90, Feb. 1988.
[16] C. S. Kuo *et al.*, "High-power harmonic gyro-TWT's—Part I: Linear theory and oscillation study," *IEEE Trans. Plasma Sci.*, vol. 20, p. 155, 1992.
[17] Q. S. Wang, D. B. McDermott, and N. C. Luhmann Jr., "Operation of a stable 200 KW second-harmonic gyro-TWT amplifier," *IEEE Trans. Plasma Sci.*, vol. 24, p. 700, 1996.
[18] M. Blank *et al.*, "Demonstration of a 10 kW average power 94 GHz gyro-klystron amplifier," *Phys. Plasmas*, vol. 6, 1999.
[19] B. G. Danly *et al.*, "Development and testing of a high average power, 94 GHz gyro-klystron", to be published.
[20] W. B. Herrmannsfeldt, "Electron trajectory program," SLAC, Stanford, CA, Rep. 226, 1979.
[21] K. T. Nguyen *et al.*, "Electron gun and collector design for 94 GHz gyro-amplifiers," *IEEE Trans. Plasma Sci.*, vol. 26, p. 799, 1998.
[22] J. J. Choi *et al.*, "Experimental investigation of a high power, two-cavity, 35 GHz gyroklystron amplifier," *IEEE Trans. Plasma Sci.*, vol. 26, p. 416, 1998.
[23] C. Liu, T. Antonsen, Jr., and B. Levush, "Simulation of the velocity spread in magnetron injection guns," *IEEE Trans. Plasma Sci.*, vol. 24, p. 982, 1996.

Khanh T. Nguyen received the B.S. degree in physics and mathematics in 1978, the M.S. degree in mathematics in 1979, and the M.S. and the Ph.D. degrees in nuclear science in 1980 and 1983, respectively, all from the University of Michigan, Ann Arbor. His Ph.D. research topic was a stability study of the ELMO Bumpy Torus Fusion Device.

He joined the Department of Research and Technology, Naval Surface Warfare Center, White Oak, where he was the Lead Theorist for the charged particle beam propagation experimental program. In 1989, he joined the Washington Office of Mission Research Corporation as a Senior Scientist, and later became the Leader of the Electromagnetic Application Group. At MRC, his research efforts were in the areas of charged particle beam propagation, vacuum electronics, compact accelerator development, x-ray and g-ray simulators, and high-power microwave sources development. Since 1994, when he initiated KN Research, he has been an on-site contractor with the Vacuum Electronics Branch, Naval Research Laboratory, Washington, DC. His current research emphasis is on the design and modeling of vacuum electronic devices.

Jeffrey P. Calame received the B.S. degree in electrical engineering and the M.S. and Ph.D. degrees in electrophysics from the University of Maryland, College Park, in 1985, 1986, and 1991, respectively.

He was an Assistant at the U.S. Naval Academy from 1980 to 1985, investigated the electrical behavior of ionic crystals and ion-conducting polymers. His graduate research from 1985 to 1991 involved the development of high peak power gyroklystrons, for which he received the APS award for Outstanding Doctoral Thesis Research in Beam Physics. From 1991 to 1992, he worked with microfabricated field emission electron sources and devices at the Naval Research Laboratory (NRL), Washington, DC. From 1992 to 1997, he studied high power microwave amplifiers, microwave processing of materials, and dielectric properties of ceramics at the Institute for Plasma Research, University of Maryland. He is currently with NRL, developing high average power, wideband millimeter wave amplifiers for radar applications.

Dean E. Pershing received the B.S. and the Ph.D. degrees in physics from North Carolina State University, Raleigh, in 1971 and 1980, respectively.

In 1980, he continued research on the generation and propagation of intense electron and ion beams as an NRC/NRL Post-Doctoral Research Associate while participating in the Naval Research Laboratory Ion Ring Program. From 1981 to 1983, he participated in the design of the Modified Betatron Accelerator at NRL, while a Staff Member of JAYCOR. Since joining Mission Research Corporation, Newington, VA, in 1983, his research has concentrated on the design and testing of high-power microwave amplifiers, including ubitron/FELs and, most recently, gyroklystrons and gyro-TWTs.

Bruce G. Danly received the B.A. degree from Haverford College, Haverford, PA, in 1978, and the Ph.D. degree in physics from the Massachusetts Institute of Technology (MIT), Cambridge, in 1983.

From 1983 to 1995, he was on the Research Staff of the Plasma Fusion Center, MIT, where his research included work on high-power gyrotrons, free-electron masers, and relativistic klystrons, along with high gradient accelerators. In 1992, he was promoted to the position of Principal Scientist at the MIT Plasma Fusion Center. In September 1995, he joined the Naval Research Laboratory (NRL), Washington, DC, as Head of the High Power Devices Section of the Vacuum Electronics Branch, Electronics Science and Technology Division. In his present capacity, he serves as Head of the Experimental Activities in the area of high-power microwave and millimeter wave generation within the Vacuum Electronics Branch.

Dr. Danly is a member of the American Physical Society, Division of Physics of Beams.

Morag Garven received the B.Sc. (with honors) and Ph.D. degrees in physics from the University of Strathclyde, Glasgow, U.K., in 1989 and 1994, respectively.

After post-doctoral work at the University of Strathclyde, she joined the Vacuum Electronics Branch of the Naval Research Laboratory (NRL), Washington, DC, in 1995, as an On-Site Contractor with the University of Maryland, College Park. Since 2000, she has been working in the Vacuum Electronics Branch, NRL, as an On-Site Contractor with Omega-P, Inc. Currently, she is investigating experimental high-power microwave devices, including gyroklystrons and gyro-TWTs.

Dr. Garven is a member of the American Physical Society.

Baruch Levush (SM'88) received the M.Sc degree in physics from Latvian University, Riga, Latvia, in 1972, and the Ph.D. degree in physics from Tel-Aviv University, Israel, in 1981.

He received Dr. Ch. Weizman Postdoctoral Fellowship and stayed for two years at University of Maryland, College Park. From 1984 to 1985, he was a Research Scientist with Rafael Research Laboratory, Israel. In 1985, he joined the University of Maryland, where his research has focused on the physics of coherent radiation sources and the design of high-power microwave sources, such as gyrotrons, TWTs, BWOs, and free electron lasers. In 1993, he became a Senior Research Scientist at the Institute of Plasma Physics, University of Maryland. In 1995, he joined the Naval Research Laboratory, Washington, DC, as Head of the Theory and Design Section, Vacuum Electronics Branch. He is actively involved in developing theoretical models and computational tools for analyzing the operation of existing microwave vacuum devices and in inventing new concepts for high power, high frequency coherent radiation sources. He is the author and co-author of over 100 journal articles.

Dr. Levush is a member of the American Physical Society.

Thomas M. Antonsen, Jr. (M'87) was born in Hackensack, NJ, in 1950. He received the B.S. degree degree in electrical engineering in 1973, and the M.S. and Ph.D. degrees in 1976 and 1977, all from Cornell University, Ithaca, NY.

He was a National Research Council Post-Doctoral Fellow at the Naval Research Laboratory, Washington, DC, in 1976 and 1977, and a Research Scientist in the Research Laboratory of Electronics, Massachusetts Institute of Technology, Cambridge, from 1977 to 1980. In 1980, he joined the University of Maryland, College Park, where he joined the faculty of the Departments of Electrical Engineering and Physics in 1984. He is currently Professor of Physics and Electrical Engineering. He has held visiting appointments at the Institute for Theoretical Physics, University of California, Santa Barbara, the Ecole Polytechnique Federale de Lausanne, Switzerland, and the Institute de Physique Theorique, Ecole Polytechnique, Palaiseau, France. His research interests include the theory of magnetically confined plasmas, the theory and design of high power sources of coherent radiation, nonlinear dynamics in fluids, and the theory of the interaction of intense laser pulses and plasmas. He is the author and co-author of over 180 journal articles and co-author of the book *Principles of Free-Electron Lasers*. He has served on the editorial board of *Physical Review Letters*, *The Physics of Fluids*, and *Comments on Plasma Physics*.

Dr. Antonsen was elected Fellow of the Division of Plasma Physics of the American Physical Society in 1986.